 FDMP, vol.12, no.2, pp.55-67, 2016

Thermal Behavior of a U-Shaped Channel Subject to a Convective Air Jet and Immersed in an Isothermal Medium

Meryem NAOUM[1] and Mustapha EL ALAMI[2]

Abstract: A numerical study of mixed convection from a U-shaped channel is carried out. The flow is considered two dimensionnel. The inlet opening is adjusted in the right vertical part of the channel, while the outlet one is placed on the left vertical part. Navier-Stokes equations are solved using a control volume method and the SIMPLEC algorithm is considered for the treatment of pressure-velocity coupling. Special emphasis is given to detail the effect of the Reynolds and Rayleigh numbers on the heat transfer generated by mixed convection. The results are given for the parameters of control as, Rayleigh number ($5.10^3 \leq Ra \leq 10^7$), Prandtl number (Pr=0.72), the hight of the vertical walls (h=5) and Reynolds number ($100 \leq Re \leq 700$). The results show that the flow structure and the heat transfer depend significantly on the inlet opening boundary conditions. Two principal kinds of the problem solution have emerged. Significant correlations are proposed related to the Nusselt number variation with Re or with Ra.

Keywords: Mixed convection, U-shaped channel, rayleigh number, prandtl number, nusselt number

Nomenclature

d	diameter of the channel (m)
D	dimensionless diameter of the channel (D=1)
h	height of the vertical part of the channel
H	dimensionless height of the vertical part
L	dimensionless length of the channel
n	normal coordinate
Nu	mean and normalized Nusselt number
Pr	Prandtl number ($Pr=\nu/\alpha=0.72$)
Ra	Rayleigh number ($Ra=g\beta\Delta TH^3/(\alpha\nu)$
Re	Reynolds number ($Re= V_0.d/\nu$)
T	temperature of fluid (K)
T_0	reference temperature (outside air (K))
t	time (s)
τ	dimensionless time ($= t.\ d^2/\alpha$)

[1, 2] LPMMAT Groupe de thermique, Faculté des sciences, Université Hassan II- Casablanca, BP 5366 Maarif, Casablanca, Morocco.

θ	dimensionless temperature of fluid (= $(T-T_f)/(T_C-T_0)$
u, v	velocities in x and y directions
U, V	dimensionless velocities in x and y directions [=(u, v)/V_0]
V_0	average jet velocity at entrance (m/s)
x, y	dimensionless Cartesian coordinates
α	thermal diffusivity
β	volumetric coefficient of thermal expansion (K^{-1})
λ	thermal conductivity of fluid (W/m.K)
ν	kinematic viscosity of fluid (m^2/s)
ρ	fluid density (kg/m^3)
ψ	stream function (m^2/s)
Ψ	dimensionless stream function(=ψ/α)

Subscripts

C	hot
f	cold
0	reference
moy	average

1 Introduction

High performance thermal systems are of interest in several engineering applications and therefore, this leads to developing techniques for heat transfer enhancement in order to reduce overall heat exchanger dimensions and to increase their efficiency. Study of convective flows in a channel shaped "U" is of practical interest in various fields, such as air conditioning to its pre-cooling, the so-called underground heat exchanger. This latter has often been the subject of several experimental and numerical studies in recent years. It helped to establish rules and reliable design tools for different configurations [Hollmuller (2002)]. Geometry improvements have also helped to optimize energy efficiency.

Significant work has been done in this subject. In particular, the work of Dehina [Dehina and Mokhtari (2012)] which proposed a numerical simulation of air-ground exchanger to improve energy efficiency; the author incorporated a coaxial tube of smaller section carrying water to irrigation at constant temperature. Naili et al. (2010) have studied the opportunity to exploit the thermal inertia of the ground for heating: An analytical study validated by experimental another was used to assess the thermal performance and optimize the heat exchanger operating parameters. Mebarki et al. (2012) studied a underground heat exchanger air conditioning system in arid areas. They studied the influence of geometrical parameters on the temperature inside the heat exchanger. KHABBAZ et al. (2014)conducted an experimental study of thermal performance of an air-ground heat exchanger (EAHX), "Canadian Well" paired with a house on the outskirts of Marrakech (Morocco). The exchanger consists of 3 PVC pipes length 77 m each buried at

a depth of 2 m to 3 m in the garden of the house. The results show that the Canadian system is well suited for the cooling of air in buildings in Marrakech, as it provides an almost constant air temperature of about 24°C when the outside temperature is between 22°C and 40°C.

In this work, we study mixed convection flows in a U-shaped channel simulating a Canadian well immersed in an isotherm soil warmer than the ambient air. The originality of this work is the introduction of several control parameters influencing the flow and heat transfer in the channel. On the other hand the different types of boundary conditions that we will study later, in same configuration, will value more our approach. First, we present results in terms of flow structure (streamlines and isotherms) for different values of the control parameters. Average temperature and velocity at the exit of the channel as well as the Nusselt number are also determined and analyzed according to the main parameters of our study. Our approach will be based on the finite volume technique.

2 Studied configuration and mathematical formulation

The studied configuration is shown in Figure 1. This is a U-shaped channel ventilated by outdoor air in the inlet (right opening) at a cold temperature (Tf, θ=0). The channel is immersed in an isotherm medium, hotter than air at the entrance. So it walls are maintained at a hot temperature (TC, θ=1).

We assume that the flow and heat transfer are two-dimensional and that the physical properties of the air are constant. The study is conducted under the Boussinesq approximation whose validity is checked for this type of system for which the maximum difference of temperature varies from few degrees Celsius to about 20 to 30°C depending on the region, the period and depth.

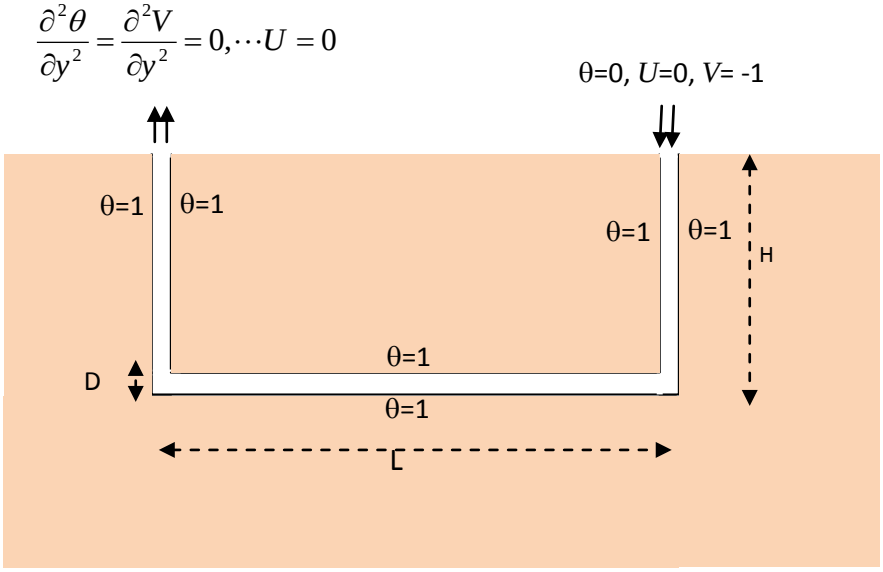

Figure 1: Studied configuration

Referring to Figure 1, the non dimensional variables are defined as follows:

$$l = \frac{L}{d},\ h = \frac{H}{d},\ \tau = \frac{t}{d/Vo},\ U = \frac{u}{Vo},\ V = \frac{v}{Vo},\ P = \frac{P}{\rho Vo^2},\ \theta = \frac{T-T_f}{T_C-T_f}$$

With:

d: Characteristic diameter, d/Vo: Characteristic time: ρVo^2 Feature Pressure, Vo: Characteristic velocity (imposed on the channel inlet).

So the non dimensional equations in terms of temperature θ, driving pressure P and velocities U and V, are written in the form:

$$\frac{\partial U}{\partial X} + \frac{\partial V}{\partial Y} = 0 \quad (1)$$

$$\frac{\partial U}{\partial \tau} + U\frac{\partial U}{\partial X} + V\frac{\partial U}{\partial Y} = -\frac{\partial P}{\partial X} + \frac{1}{Re}\left(\frac{\partial^2 U}{\partial X^2} + \frac{\partial^2 U}{\partial Y^2}\right) \quad (2)$$

$$\frac{\partial V}{\partial \tau} + U\frac{\partial V}{\partial X} + V\frac{\partial V}{\partial Y} = -\frac{\partial P}{\partial Y} + \frac{1}{Re}\left(\frac{\partial^2 V}{\partial X^2} + \frac{\partial^2 V}{\partial Y^2}\right) + \frac{Gr}{Re^2}\theta \quad (3)$$

$$\frac{\partial \theta}{\partial \tau} + U\frac{\partial \theta}{\partial X} + V\frac{\partial \theta}{\partial Y} = \frac{1}{RePr}\left(\frac{\partial^2 \theta}{\partial X^2} + \frac{\partial^2 \theta}{\partial Y^2}\right) \quad (4)$$

The boundary conditions associated with these equations are defined as:

- At the inlet opening of the channel : θ=0, V= -1 , U=0
- At the channel outlet: U=0, $\frac{\partial^2 \theta}{\partial Y^2} = 0$, $\frac{\partial^2 V}{\partial Y^2} = 0$ [6,7]
- On the walls: U=V=0, θ=1

3 Numerical method

The results presented in this work, have been obtained by using numerical procedure based on a finite volume technique [Patankar (1980)]. The governing equations were solved considering the boussinesq approximation. Two dimensional flows are considered in this study and the velocity-pressure coupling is solved by using SIMPLEC algorithm [Van Doormaal and Raithby (1984)].

As a result of a grid independence study, a grid size of 80x160 was found to model accurately the flow fields described in the corresponding results. Time steps considered are ranging between 10^{-4} and 10^{-3}.

The accuracy of the numerical model was verified by comparing our results with those obtained by De Val Devis (1983) and Le Queré, Alziary De Roquefort (1985) for natural convection in differential heated cavity, Table 1, and then with the results obtained by Kalache et al. (1985) in a trapezoidal cavity (Table 2).

Finally, we have confronted our results to those proposed by Derayaud and Fichera [Desrayaud and Fichera (2002)] in a vertical channel with two ribs symmetrically placed on the channel walls (Table 3). Good agreement was obtained in Ψ_{max} and *Nu* terms. When a steady-state is reached, all the energy furnished by the hot wall to the fluid must leave the channel through the outlet opening. This energy balance was verified by less than 3% in all cases considered here.

Table 1: Comparison of our results and those of De Val Devis et al. (1983), Le Queré et al. (1985).

Ra	De Val Devis et al. [De Vahl Davis (1983)]	Le Queré et al.[Le Queré et al. (1985)]	Present study	Maximum deviation
10^4	Ψ_{max}= 5.098	-----	Ψ_{max}=5.035	1.2%
10^5	Ψ_{max}=9.667	-----	Ψ_{max}=9.725	0.6%
10^6	Ψ_{max}=17.113	16.8110	Ψ_{max}=17.152	0.2%
10^7	------	30.170	Ψ_{max}=30.077	0.3%

Table 2: Comparison of our results and those of Kalache et al. (1985)

Gr	Present study	Kalache et al.	Maximum deviation
2.5×10^3	Ψ_{max}=5.42	Ψ_{max} =5.37	2.4 %
5×10^3	Ψ_{max} =9.74	Ψ_{max} =9.77	4.1 %
10^4	Ψ_{max} =15.43	Ψ_{max} =15.41	0.2%

Table 3: Comparison of our results and those of Derayaud and Fichera (2002).

Ra=10^5 (A=5)	Derayaud and Fichera.	Present study	Maximum deviation
Ψ_{max}	151.51	152.85	0.9%
M	148.27	151.72	2.2%

4 Results and discussion

In this paper, the analysis is focused on heat transfer rate across the hot walls, flow and thermal fields for range of *Rayleigh* number: $5x10^3 \leq Ra \leq 10^7$, *Reynolds* number: $100 \leq Re \leq 700$ and other parameters of the problem (L=10, D=1, H=5 and Pr=0.72). *Rayleigh* number values and Reynolds number ranges are chosen in favour of mixed convection role.

The particularity of this problem is the appearance of different solutions when varying the parameters Re and Ra. The flow structure is, essentially, composed of the open lines, which represent the forced flow, and closed cells which are due to the recirculating movement up of the jet or to natural convection phenomena. In this later case, the cells are dawn of the forced flow, localised substantially in the right column of the channel.

In this section, we present the effect of the control paramter variations on the flow structure and the thermal field. These will be presented as streamlines and isotherms for the following values:

- Reynolds number variation: $100 < Re < 700$, $R=10^5$, Pr=0.72, d=0.2m, L=10, H=5
- Rayleigh number variation : $10^3 < Ra < 10^7$, Re=500, Pr=0.72, d=0.2m, L=10, H=5

4.1 Qualitative study

4.1.1 Reynolds number variation

In this paragraph, we discuss the Reynolds number effect on the flow structure and heat

transfer. We have identified two main areas of the Reynolds number in the range 100≤ Re ≤ 700: An area of low values of Re (100≤Re≤500) for which Nu increases with Re. A second zone of large values of Re (500≤Re≤700) in which Nu decreases when Re increases.

Only typical representative figures of the flow structure will be presented in this paper.

For low values of Reynolds, the streamlines are almost parallel to each other and to the walls of the channel, Figure 2, for Re=300. The boundary lines prokatyvajut walls except in the lower corners of the channel, where these is flow separation. So, we get a simple structure. The thermal field (left) shows that the heat exchange between the walls and the ventilation jet of fresh air is mainly performed in the vertical column on the right. Indeed, the velocity of ventilation at the inlet is still weak (and therefore low mass flow rate) and favors a limited heat transfer in a vertical air intake column. We note that in the rest of the channel, there is practically no heat exchange between the active walls and the inside air. Increasing Re, a flow contraction zone appears at the corners, Figure 3 and 4, for Re=400 and 500, respectively. The one on the right corner is stronger than the left. This may be due to the reversal of the flow direction (opposite to gravity in the right corner and the contrary, in the left corner). Note also that the two modes of natural convection and forced convection operate in the opposite direction (right column) and in the same direction (left). Narrowing zones are increasing progressively, as Re increases, until appearance of the recirculating cells at the two corners, Figure 5, Re=600. The structure of the flow becomes relatively complex.

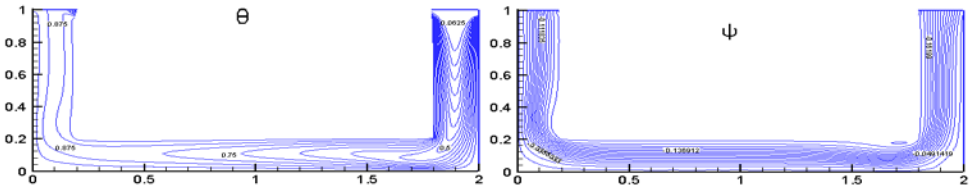

Figure 2: Isotherms and Streamlines for Re=300, Ra=10^5

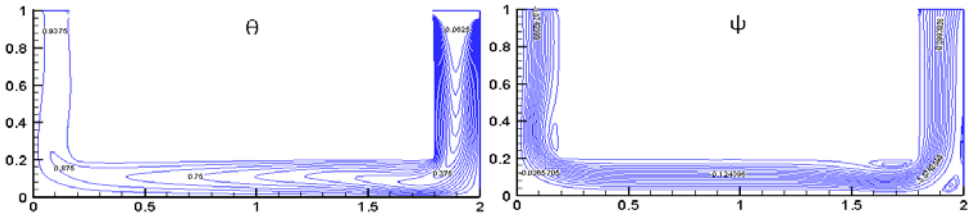

Figure 3: Isotherms and Streamlines for Re=400, Ra=10^5

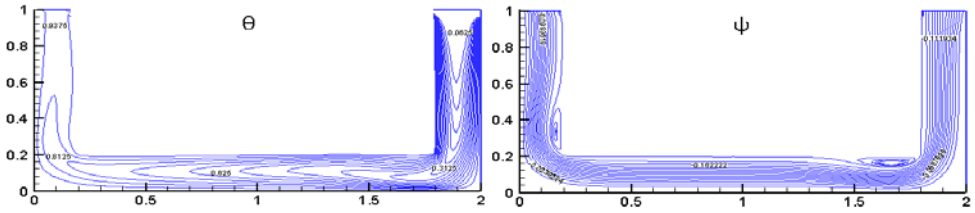

Figure 4: Isotherms and Streamlines for Re=500, Ra=10^5

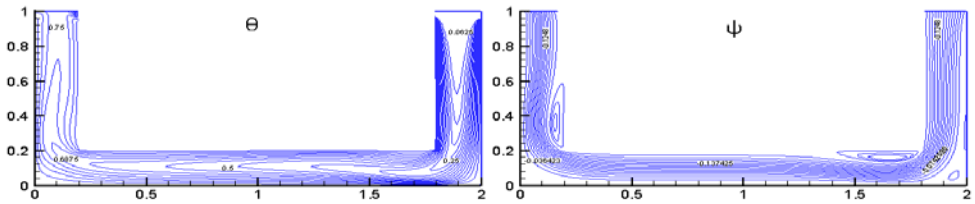

Figure 5: Isotherms and Streamlines for Re=600, Ra=105

4.1.2 Rayleigh number variation

We set the Reynolds number around its optimal value Re=500 (obtained in the exploration of the preceding paragraph) and we varied Rayleigh number in the following range related to the laminar flows: $10^3 \leq Ra \leq 10^7$.

For Low Rayleigh number ($10^3 \leq Ra \leq 10^4$), the flow structure is identical to that shown in Figure 6, for $Ra=10^4$. Streamlines are almost parallel to each other and parallel to the channel walls. By cons, they have small deviations at the corners and the left vertical column and then laminated with the walls of the left vertical column. We also note a slight gap between the streamlines and channel walls. It is probably due to the flow separation at the levels of the two corners thereof. The thermal field (left) shows a very marked isothermal tightening along the walls of the vertical inlet column and on the right side of the horizontal walls. Heat Exchange between the hot medium and the air is getting, mainly, at the first half of the channel. For $Ra=10^5$ (case treated in the previous paragraph, Figure 4) the structure of the flow is substantially identical to the case of $Ra=10^4$, with a slight increase of the recirculating cells into the corners of the channel. Above $Ra=10^5$, the air flow has significant changes in thermal and dynamic fields. Indeed, for $Ra=10^6$, Figure 7, the streamlines lose their simple structure, in particular, we note the intensification of the two training cells located above the air jet and the emergence of a second cell down of the fresh air jet and in the right corner of the channel. The latter causes a substantial separation of the forced jet of fresh air, along the entire vertical wall of the right vertical channel part. This separation occurs in a negative way on the heat transfer between the wall and the fresh air: the isothermal lines are distorted and relatively dispersed in this area, by comparison to the previous cases.

For $Ra=10^7$, Figure 8, and in comparison to thermal and dynamic fields in the previous

paragraph, two important points should be emphasized:

- The multicellular structure becomes strong in heat exchange zone (right column) where there is the appearance of convective cells in just a few areas, especially near the hot walls. We also note the increase in high heat exchange areas that stretch up to the beginning of the horizontal portion. A return flow is also observed at the exit of the channel, confirming the strong competition between forced and natural convection.
- The second point concerns the distortion of the streamlines in the horizontal part of the channel because of the thermal gradient that intensifies with increasing Ra. Heat transfer in this horizontal part becomes very important in the first half of the channel. This importance is explained by the opposition of the two convection modes, against the second part of the channel both modes operate in the same direction.

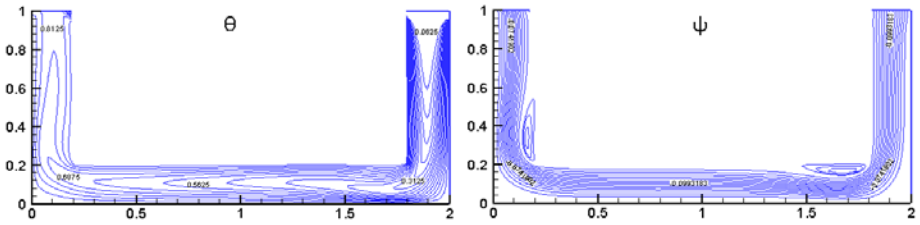

Figure 6: Isotherms and Streamlines for Re=500, Ra=10^4

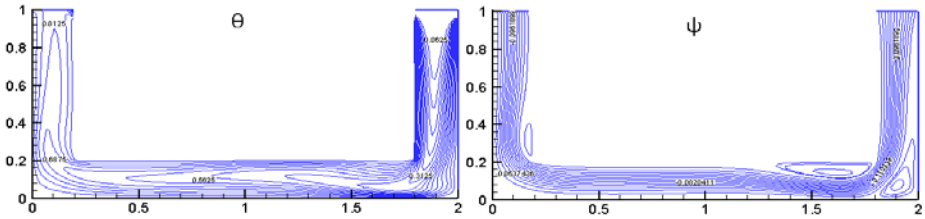

Figure 7: Isotherms and Streamlines for Re=500, Ra=10^6

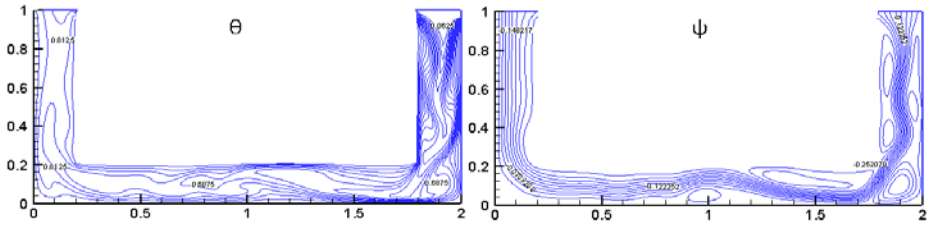

Figure 8: Isotherms and Streamlines for Re=500, Ra=10^7

4.2 Quantitative Study

We present, in this section, the effect of the Reynolds number variation on the channel outlet temperature and velocity for the value selected Rayleigh (Ra=10^5).

Knowing the velocity and temperature profiles at the exit of the channel, we gave information ons the amount of energy gained by air from entering the channel until it leaves. It is, therefore, important to examine their evolutions at this zone of channel. In Figure 5 and 6, we present the profiles θ(x) and V(x), respectively for Re=100 and Re=700. We find that along the major part of the outlet opening, air exits at a temperature close to that of thechannel walls. The outlet velocity profile, in turn, is symetric and does not exceed the value 1.4 (dimensionless velocity). When Re increases, the thermal profile becomes symmetrical for Reynolds number up to Re=300 (figure not shown) and then θ(x) is a parabola centered in the middle of the opening.

We note in these figures that the air exits cooler as Re increases and the outlet velocity becomes important. It should be noted that the study of profiles θ(x) and V(x) according to the Rayleigh number variation (Figures not shown), was performed by setting the value of the Reynolds number Re=500. These profiles are virtually identical to those of Figure 9 and 10.

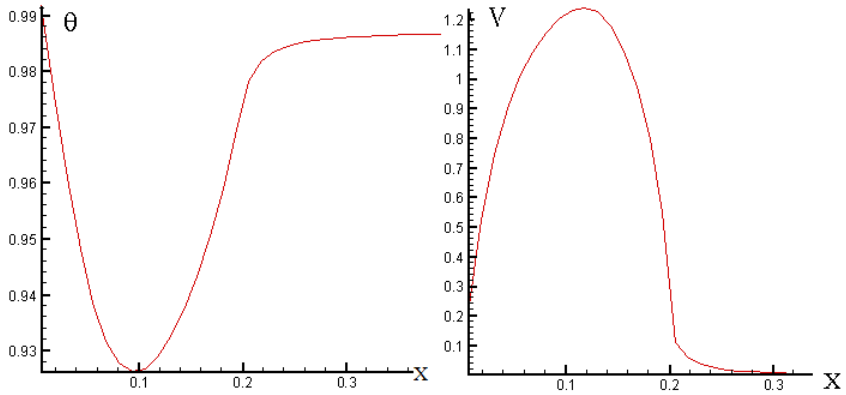

Figure 9: Temperature and velocity variation at the channel outlet for Re=100, Ra=10^5

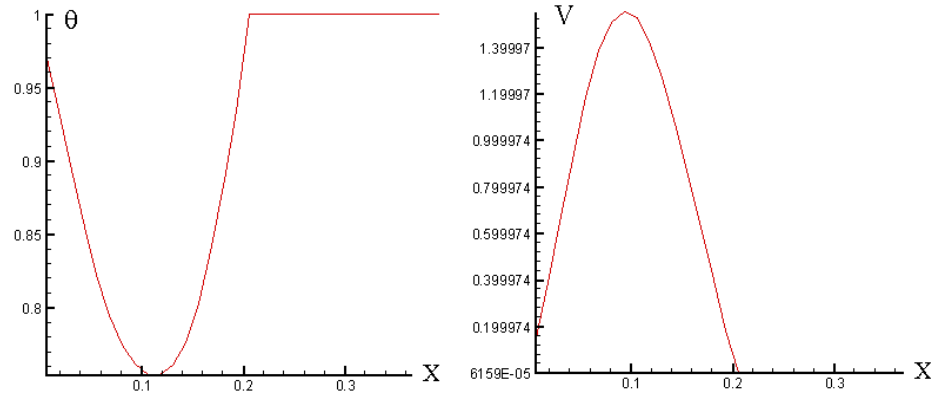

Figure 10: Temperature and velocity variation at the channel outlet for Re=700, Ra=10^5

The average values of the temperature θ_{moy} and velocity V_{moy} at the exit of the channel, are also studied by variing the principle control parameters of this work (Re and Ra).

By setting $Ra=10^5$, we find that the average temperature at the channel output remains, practically, constant around the value of $\theta_{moy}=0.88$ in the range of Reynolds number $200\leq Re\leq 500$ and then falls rapidly at $Re=600$ ($\theta_{moy}=0.75$) and increases again at $Re=700$, Figure 11.

For against, as regards the average velocity V_{moy} at the outlet of the channel, it constantly decreases from Re=100 to 600 and then increases in the range $600\leq Re\leq 700$. This leads to the conclusion that in this type of configuration, you must ventilate at low flow rates to achieve good air cooling (Figure 12).

These quantities are then studied according to the Rayleigh number as shown in Figure 13 and 14. Figure 13 and 14 are the expressings for θ_{moy} and V_{moy}, respectively. Note that the average temperature slightly varies with Rayleigh, contrary to the average velocity which remains constant in the region of low Rayleigh number, and then increases exponentially when the number of Rayleigh exceeds the value of $Ra=10^5$. This finding confirms that the air jet is energetically more powerful and therefore more cost-effective for high values of Ra. This is a trivial result since more and more thermal gap between the ground and the outside air is large, more and more heat is recovered in the pipe system.

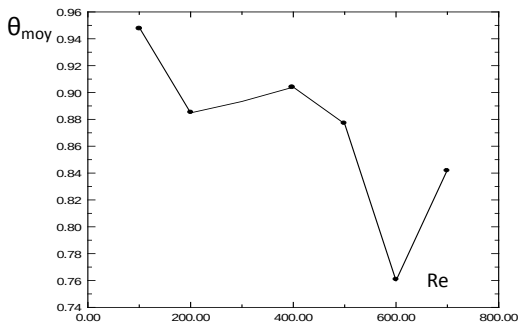

Figure 11: Average temperature Variation with Re at the channel outlet, Ra=105

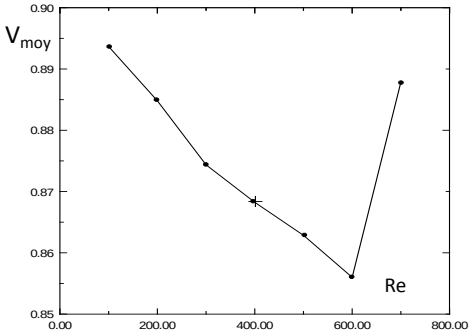

Figure 12: Average velocity Variation with Re at the channel outlet, $Ra=10^5$

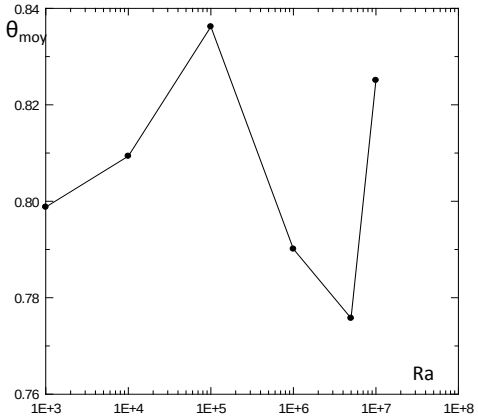

Figure 13: Average temperature variation with Ra at the channel

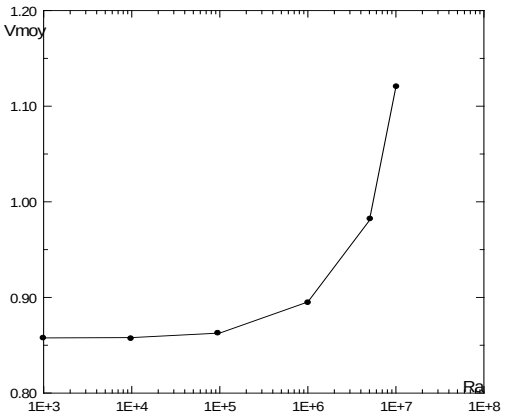

Figure 14: Average velocity variation with Ra at the channel outlet

4.3 Heat transfer

Heat exchange between the channel walls and fresh air (convective jet) is evaluated in terms of average Nusselt number. Its variation with Reynolds number is shown in Figure 11. We see that Nu increases with a logarithmic trend between Re=100 and Re=500, a value for which reaches a maximum and then fall slightly between Re=500 and 700. The value of Re=500 is presented as an optimal value in this type of configuration.

We correlated Nu *vs.* Re in the range $100 \leq Re \leq 500$ by the relationship: $Nu \approx 2.95 \times \ln(Re) - 4,9$, for $Ra = 10^5$.

This result is similar to those provided by available correlations in the literature, Abid et al. (2012) and Meskini et al. (2011). We can also note that there has been a fall in the Nusselt number curve for the high values of Re, which is also found in these two references with less intensity than the one shown in this figure (Figure 15).

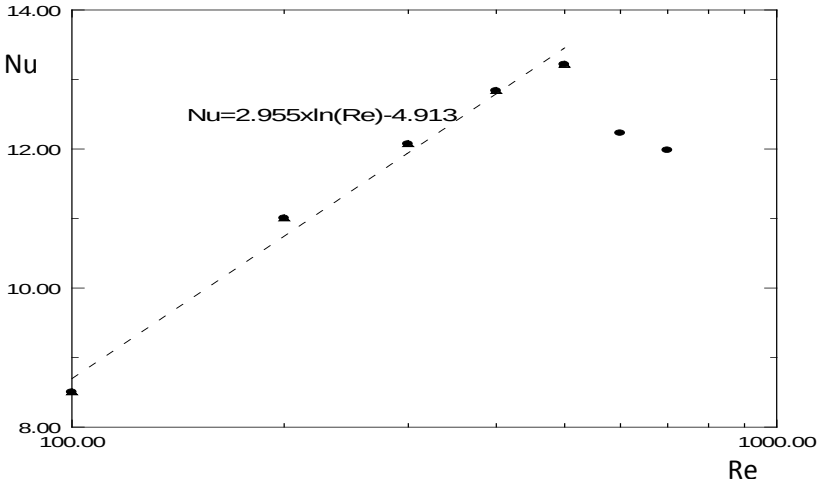

Figure 15: Nusselt number variation with Re number, $Ra = 10^5$

In the same manner, the variation of the Nusselt number with Rayleigh number is presented in Figure 16. We note that Nu decreases slightly between Ra=10^3 and 10^6 and then it increases rapidly (Nu=23.18) between 2×10^6 and 5×10^6. Maximum of Nu is sensed around the latter value of Ra. Above Ra= 5×10^6, Nu slowly falls from 23.18 to 19.62.

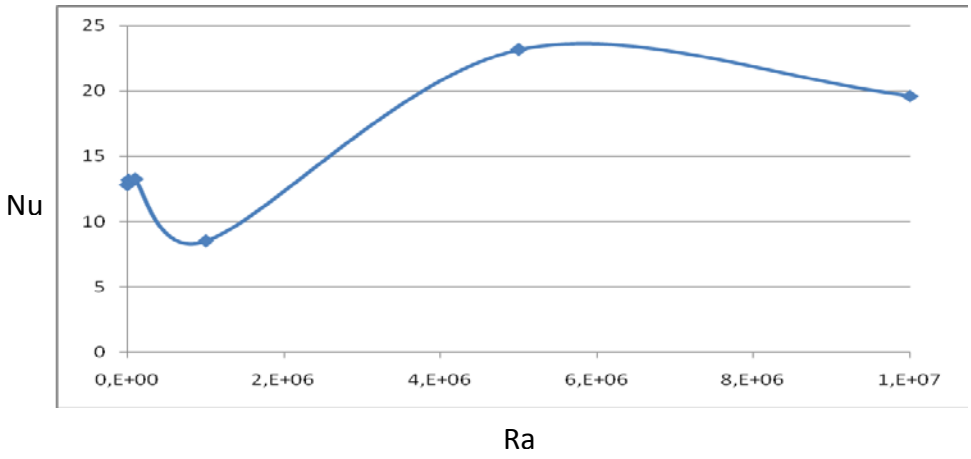

Figure 16: Nusselt number variation with Ra, Re=500

5 Conclusions

We have numerically studied mixed convection flows in a U-shaped channel which can represent a Canadian well for air cooling. We have presented in this article, the first results in terms of flow structures and heat transfer through the channel. The results show that:

- At low Re, the heat exchange is limited to the right vertical column of the channel. The major part of the channel is nearly isotherm,
- When Re increases, there is significant improvement of heat exchange along all the walls of the channel,
- If one continues to increase Re, drive cells appear and cause a flow separation at the corners of the channel, which destroyed the transfer of heat from hot isotherm medium to fresh air,
- The Nusselt number has a maximum around the value Re=500 in the case where the Rayleigh number is set equal to Ra=10^5,
- At low values of Ra, the drive cells appear in the corners and at the outlet of the channel and continue to increase in size to occupy all parts of the channel for high Ra.

As a result significant in engineering, we have proposed a correlation of Nusselt number versus Re. By cons, we could not correlate the variation of Nu according to Ra, since the latter has an oscillatory appearance.

Acknowledgment: This work is a part of RafriBat project. Authors acknowledge the financial support provided by l'Académie Hassan II des Sciences et Techniques, Morocco.

References

Abid, Y.; Meskini, A.; Najam, M.; El Alami, M. (2012): Electronic Component Cooling by mixed convection: Block Size Effects . *Physical and Chemical News*, vol. 65, pp. 22-28.

De Vahl Davis, G. (1983): Natural convection of air in a square cavity: a bench mark numerical solution. *International journal of numerical methods in fluid*, vol. 3, pp. 249-264.

Desrayaud, **G.**; **Fichera**, **A.** (2002): Laminar natural convection in a vertical isothermal channel with symmetric surface mounted rectangular ribs. *International Journal of Heat and Fluid Flow*, vol. 23, pp.519-29.

Dehina, K.; Mokhtari, A. M. (2012): Simulation numérique d'un échangeur air-sol-eau à co-courant. XXX^{e} Rencontres AUGC-IBPSA Chambéry, Savoie, 6 au 8 juin.

El Alami, M.; Semma, E. A.; Najam, M.; Boutarfa, R. (2009): Numerical Study of Convective Heat Transfer in a Horizontal Channel. *Fluid Dynamics & Materials Process*, vol. 5, no. 1, pp. 23-36.

Hollmuller, P. (2002): *Utilisation des échangeurs air/sol pour le chauffage et le rafraichissement des bâtiments*. Thèse de Doct., Université de Genève.

Kalache, D.; Penot, F.; Le Quéré, F. (1985): Numerical investigation of the validity of the two-dimensional assumption in the computation of natural convection within a trapezoidal cavity Num. Methods in laminar and turbulent flow. *4th International Conference, Swansea*, UK, pp. 829-840.

Khabbaz, M.; **Benhamou, B.**; **Limam, K.; Hamdi, H.; Bennouna, A.; Hollmuller, P.** (2014): Etude expérimentale d'un échangeur de chaleur air-sol (puits canadien) pour le rafraichissement d'un bâtiment résidentiel à Marrakech: 3ème congrès international de thermique AMT'2014, 21 et 22 Avril 2014, Agadir, Morocco.

Le Queré, P. ; **De Roquefort, T. Alziary** (1985): Computation of natural convection in twodimensional cavities with chebyshev polynomials. *Journal of Computational Physics*, vol. 57, pp. 210-228.

Meskini, Ahmed; Najam, Mostafa; El Alami, Mustapha (2011): Convective mixed heat transfer in a square cavity with heated rectangular blocks and submitted to a vertical forced flow. *Fluid Dynamics & Materials Process*, vol. 7, pp. 97-110.

Mebarki, B.; **Draoui, B.**; **Abdessamad, S.**; **Keboucha, A.**; **Drici**, **S.**; **Sahli, A.** (2012) : Étude d'un système de climatisation intégrant un puits canadien dans les zones arides, cas de Béchar. R*evue des Énergies Renouvelables*, vol. 15, no. 3, pp. 465-478.

Mahrouche, O.; Najam, M.; El Alami, M.; Faraji, M. (2012): Mixed Convection Investigation in an opened Partitioned Heated Cavity. *Fluid Dynamics & Materials Process*, vol. 9, no. 3, pp. 235-250.

Nali, N.; Kooli, S.; Ferhat, A. (2010) : Optimisation analytique et validation expérimentale d'un échangeur enterré. *Revue des Énergies Renouvelables*, vol. 13, no. 3, pp. 525-535.

Patankar, S. V. (1980): *Numerical heat transfer and fluid flow*, McGraw-Hill.

Van Doormaal, J. P.; Raithby, **G. D. (**1984): Enhancements of the SIMPLE method for predicting incompressible fluid flows. *Numerical Heat Transfer*, vol. 7, pp. 147-163.